



Development of laser ultrasonics inspection for online monitoring of additive manufacturing

Célia Millon¹ · Arnaud Vanhoye¹ · Anne-Françoise Obaton² · Jean-Daniel Penot¹

Received: 11 September 2017 / Accepted: 6 February 2018 / Published online: 21 February 2018
© International Institute of Welding 2018

Abstract

The quality control of additive manufacturing (AM) parts and the repeatability of AM process are critical issues for the widespread of AM especially for aerospace and healthcare sectors. Due to production costs, there is a strong interest in reducing scrap rates and process monitoring. Laser ultrasonics is a promising technology that fits the constraints of AM online monitoring. This technique shows potential for inspecting the upper cord of the part during manufacturing, as it is a non-contact and nondestructive testing. The generation is produced by a brief laser impulse which heats up the material, inducing constraints that release into ultrasonic waves. Two generation modes can be encountered using lasers: thermoelastic and ablative, depending on the energy deposited on the surface. The generated waves interact with the medium and flaws, thus allowing the detection of defects such as lack of fusion or porosities. The detection is performed using a two-wave mixing interferometer, also contactless. In this paper, we present work carried out in order to evaluate the feasibility and the effectiveness of laser ultrasonics testing for online additive manufacturing process. The influence of key parameters such as laser spot dimensions is highlighted through both experiment and modeling. We present first results obtained on additive manufactured parts containing machined notches.

Keywords Laser ultrasonics · Additive manufacturing · Online process · Direct metal deposition · Direct energy deposition

1 Introduction

This paper addresses the main metallic additive manufacturing (AM) processes: direct energy deposition (DED) and powder bed fusion. Direct energy deposition consists in focusing the energy delivered by a laser to heat powder, melting it and simultaneously melting material that is being deposited into the substrate's melt pool (cf. Fig. 1). Powder bed fusion consists in selectively melting a powder bed layer using a laser.

AM is attracting considerable interest due to all the possibilities that it offers in comparison to forging process. AM has now applications in the leading-edge sectors such as aerospace and healthcare [1]. Despite AM generating considerable interest, this is not a time-tested technology, and some limits hinder

the widespread of AM. Dimensional precision, reliability, and repeatability of the process remain questions [2–4]. Thus, on-line monitoring process, inspecting the entire piece layer by layer, is useful to implement a feedback loop which could process whenever a flaw is detected. This highlights the economic interest of such monitoring for time machining as well as saving raw material. Laser ultrasonics (LU) are a nondestructive testing technique that has been already considered for monitoring the build part after the melt pool [5]. The aim of LU inspection is to detect surface and internal flaws which appear during manufacturing.

A drift in the nozzle trajectory can lead to layers not overlapping properly and thus triggers the formation of notches or lack of fusion (cf. Fig. 2). Lacks of fusion are caused by unmelt powder and give rise to porosities. The size of these flaws does not generally exceed the thickness of a layer that is a few hundred micrometers.

Our aim is to control the upper layers of the sample by following the fabrication nozzle. We want to inspect a few millimeters depth of material, a few millimeters after the melt pool. Thus, we are focusing on surface and subsurface flaws. The most well-suited waves to do so are surface waves (Rayleigh waves), as they are generated with higher amplitude

This article is part of the collection Welding, Additive Manufacturing and Associated NDT

✉ Célia Millon
celia.millon@cea.fr

¹ Commissariat à l'Énergie Atomique, Saclay, Paris, France

² Laboratoire National de Métrologie et d'Essais, Paris, France

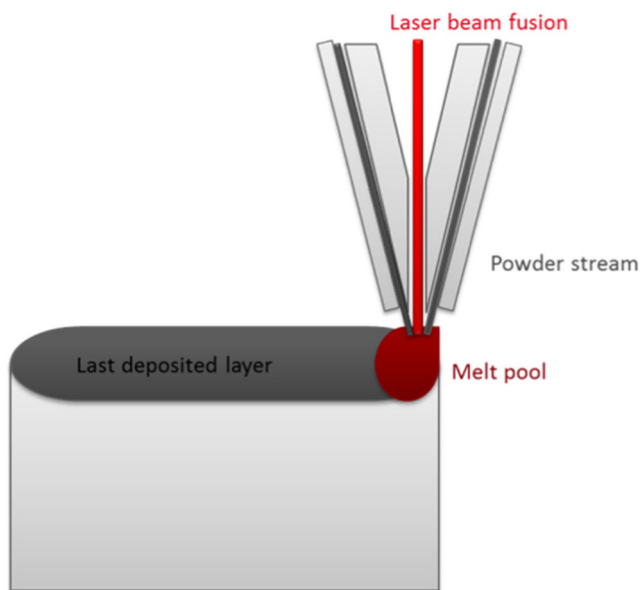


Fig. 1 Diagram of direct energy deposition

than volume waves by LU. Moreover, Rayleigh wave's depth penetration is adapted to the control depth we are aiming for.

In this paper, we present the first step towards LU integration into an AM machine that is to evaluate LU inspection for AM. After recalling the principle of the technique, the influences of the main parameters of a LU inspection are introduced to define an experimental setup for AM flaw investigations. The device is designed in accordance with models and experimental validations. Then, we present the results obtained with the experimental setup. We opted for studying a simplified case in order to identify the different acoustic signatures caused by geometry, fabrication process, or flaws.

2 Principles of laser ultrasonics inspection

LU constitutes a nondestructive testing (NDT) allowing monitoring the build parts after the melt pool, during the cooling down of the part. LU is a method to generate and detect ultrasonic signals remotely with lasers and does not require any direct physical

Fig. 2 On the left, effect of nozzle trajectory error, on the right, micrographic section of porosities in AM media (the two pieces are made by direct energy deposition)

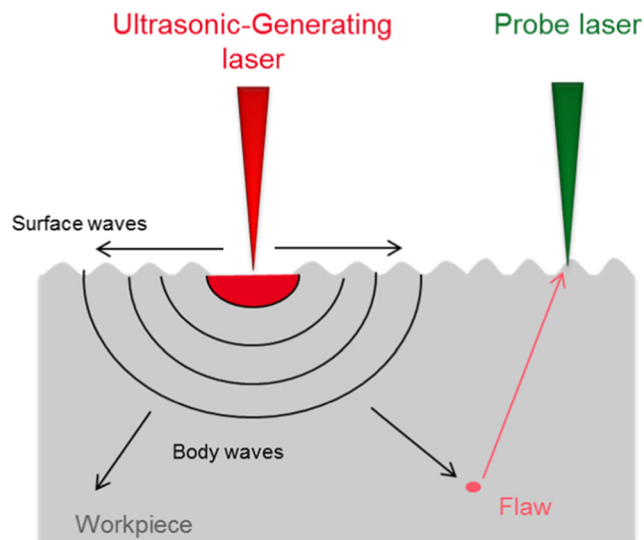
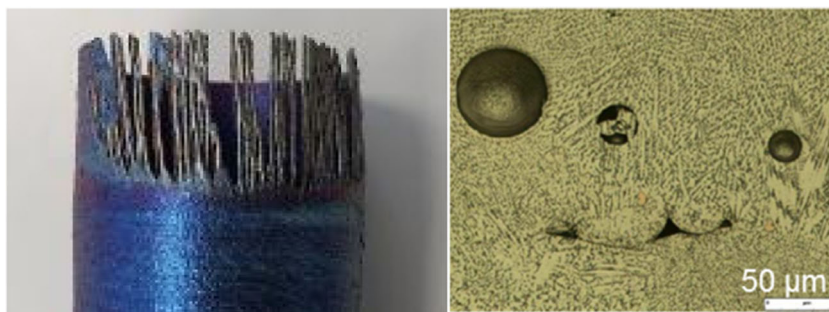


Fig. 3 Principle of laser ultrasonics inspection

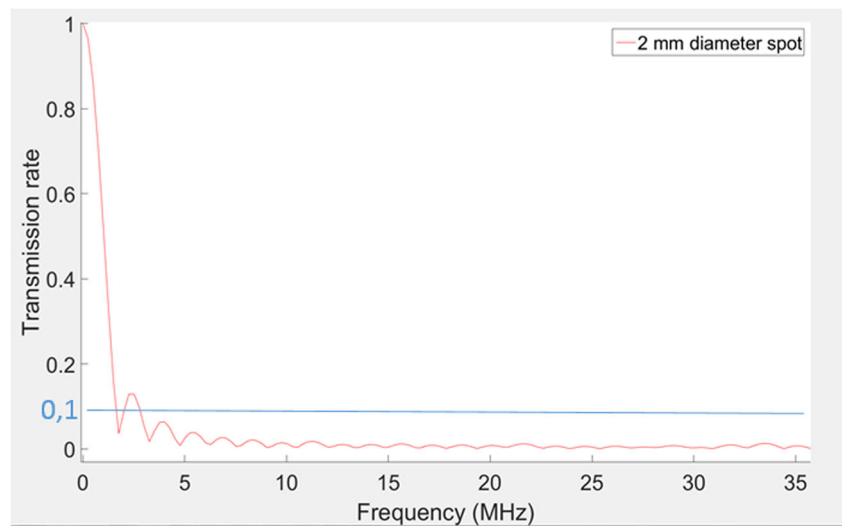
contact between probes and sample. In this way, LU is well fitted to the hot temperature encountered during the AM process.

The generation process of ultrasound by a pulsed laser is based on the interaction of light with the material [1]. The light absorption induces thermal dilatation constraints in the material that release into ultrasonic waves. There are two main generation modes depending on the energy deposited. The brief laser impulse can either lead to a reversible thermoelastic deformation (thermoelastic mode) or at higher energy induce melting and vaporization of the material (ablative mode) which is not nondestructive anymore. Our study ensured that the experiments were performed within the thermoelastic regime.

Both surface and volume elastic waves are created (respectively Rayleigh waves and compressional and transversal waves). The interactions of waves with flaws induce surface displacements which can be detected by interferometry. Figure 3 sums up the principle of LU inspection.

This technique enables both surface and subsurface inspections and expands the scope of existing monitoring control [2]. Indeed, contrary to other in situ techniques, our aim is to detect porosities and lacks of fusion occurring after the melt pool.

Fig. 4 Transmission rate frequencies for a 2-mm spot diameter



3 Experimental setup

3.1 Model-based selection of laser beam parameters

With respect to flaw sizes of interest, the wavelength of generated waves must be about 0.1 mm which corresponds to frequencies above 15 MHz for Rayleigh waves. Those values are calculated for steel wave velocities (Rayleigh waves velocity is approximately equals to 2900 m/s in steel at 20 °C). The choice of 15 MHz relates the compromise between a better resolution and an acceptable attenuation.

As part of our experiments, ultrasounds are generated by laser irradiation in the thermoelastic regime, as this regime does not deteriorate the work piece [3]. The pulse duration gives the highest possible frequency of generated waves: for an impulse of 10 ns, frequencies are in the range of 10 MHz [1]. However, during our first experiments, we observed that waves' frequencies do not exceed 3 MHz. To understand why

we have such results, we develop models to study the influence of size and shape of laser spot on the frequencies detected by the system, especially for surface waves.

Let us consider the generation (resp. detection) laser spots as a distribution of elementary emitters (resp. receivers) of brief impulses and analyze the detected frequencies when spot size is varying. We have developed a model that predicts the impact of laser beam size onto the detected frequencies. This model has been validated experimentally. Figures 4 and 5 illustrate the transmission rate of frequencies by the laser spot system for different generation laser size spots size for Rayleigh waves. We assume the detection spot is punctual.

For a 2-mm spot diameter, the transmission rate decreases drastically at 2 MHz with a transmission value lower than 20%. At 3 MHz, the transmission rate is below 10% which is a frequency content not significant enough to extract information of flaws. For this spot size, frequencies exploitable are between 0 and 3 MHz.

Fig. 5 Transmission rate frequencies for a 0.2-mm spot diameter

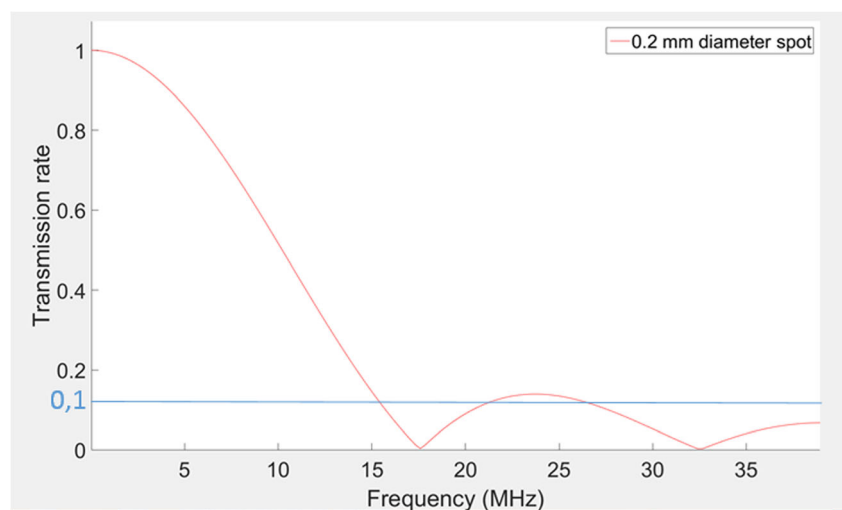
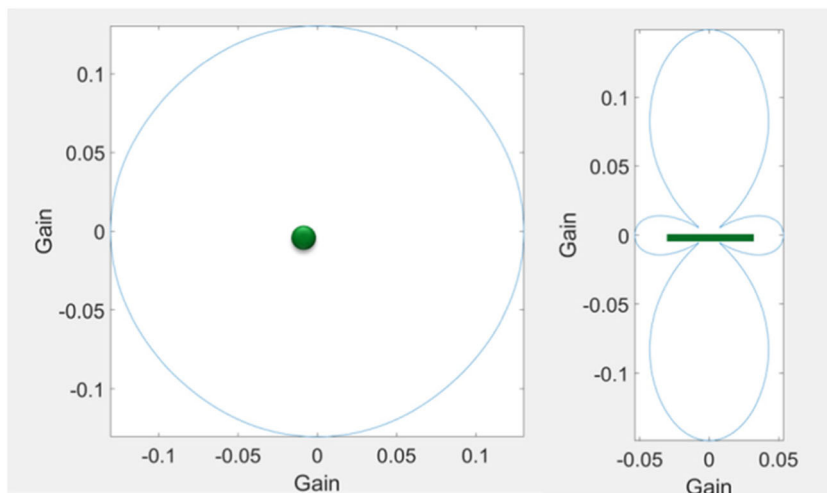


Fig. 6 Directivity diagram for Rayleigh waves in the thermoelastic regime for a circular laser spot (on the left) and a linear laser source (on the right)—frequency is 2 MHz and the detection point is at 3 mm from the source



For a 0.2-mm spot diameter, the transmission rate decreases progressively from 100 to 20% between 0 and 15 MHz. Then, the value of transmission rate is below 10% until 20 MHz. For this spot size, frequencies exploitable are between 0 and 15 MHz.

As mentioned, we need to reach 15 MHz for our application, so we must design a device that allows focusing laser beams below 0.2 mm.

Spatial dimensions of laser beams have also an impact on the wave directivity. We have modeled the directivity diagram of Rayleigh waves in steel. Figure 6 presents the directivity diagram of Rayleigh waves for a circular and for a linear spot shapes.

As shown in Fig. 6, directivity diagram of Rayleigh waves generated by a circular source is isotropic, whereas for a line source, the generated waves mainly propagate in the direction perpendicular to the laser line. We have confirmed that there is a main propagation direction when using the laser line by experimental observations as shown in Fig. 7.

In configuration 1, the detection spot is in a direction perpendicular to the laser line that is to say the best one according to the

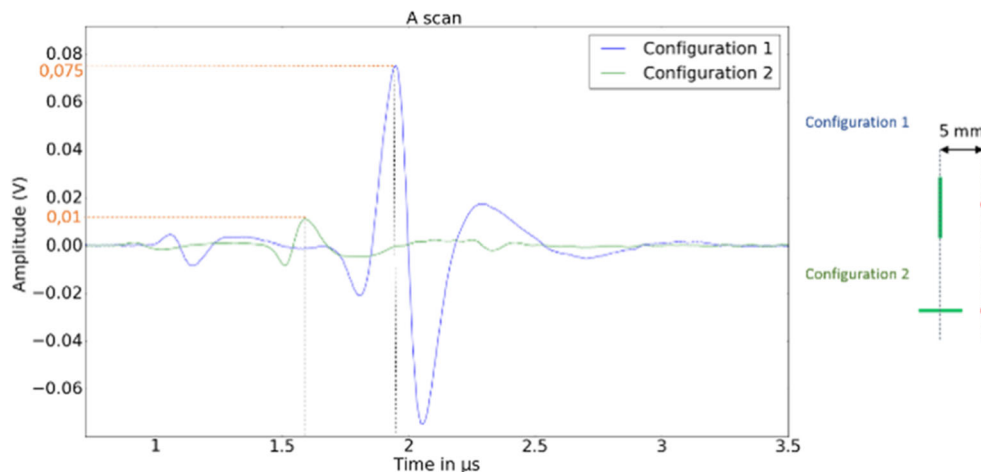
previous statement. The amplitude of Rayleigh wave is 0.075 V. In configuration 2, the detection spot is located in a direction following the laser line. The time delay between the first and second configuration is due to the distance separating generation and detection as shown in Fig. 7. The amplitude of Rayleigh wave is 0.01 in configuration 2. This proves that the main direction of propagation is perpendicular to the laser line direction as the amplitude is 17 dB higher than in configuration 2.

Consequently, the probe must be positioned along this direction. Following these conclusions, we have designed optical devices focusing the generation laser beam into a 0.2-mm width line and focusing the detection into a disk-shaped spot of 0.2 mm diameter. The optical device for generation consists of a cylindrical lens combined to an aspheric lens. A diaphragm is used to adapt the line length regarding the part dimension. Figure 8 shows the laser line focalized by the designed optical device.

In Fig. 9 is presented the spectrum of the Rayleigh wave obtain in configuration 1 (cf. Fig. 7).

Thus, we confirm by experimentation that Rayleigh waves are generated between 0 and 15 MHz.

Fig. 7 Rayleigh wave recorded along a direction perpendicular to the generation line (configuration 1) and along to a direction parallel to the generation line (configuration 2)—acquisition on aluminum sample



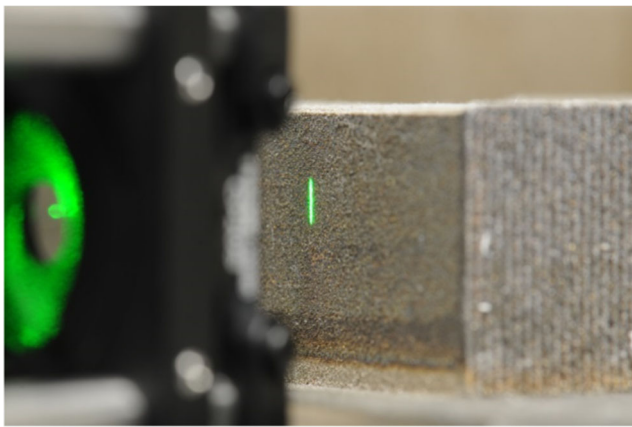


Fig. 8 Ultrasound generating laser beam focused on a AM sample

3.2 Laser ultrasonics setup

Two Nd:YAG lasers are used for ultrasound generation and detection. Generation has a mean power of 0.6 W and detection 2.5 W (both have a 20-Hz frequency). The generation laser wavelength is 532 nm, the pulse duration is 7 ns, and the energy provided by each pulse is 30 mJ. The probe laser wavelength is 1064 nm, and the pulse duration is 80 μs. The interferometer is a two-wave mixing interferometer made of a photorefractive crystal [6]. Figure 10 shows the laser ultrasonics setup and the optical device developed to focus laser beams.

Laser beams are injected into fibers which carry them to the optical device in order to be focused. The two lasers are positioned on the same face of the sample to exploit Rayleigh waves and the LU system scans the sample. The power density delivered to the sample is about 7 MW/cm², and no marks of the heating are visible so that the generation mode could be considered as thermoelastic.

The next paragraph gives information about the tested samples.

Fig. 9 FFT of Rayleigh wave—aluminum sample configuration 1

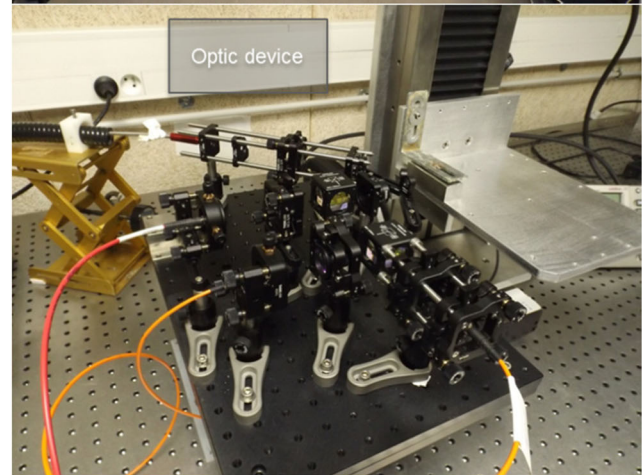
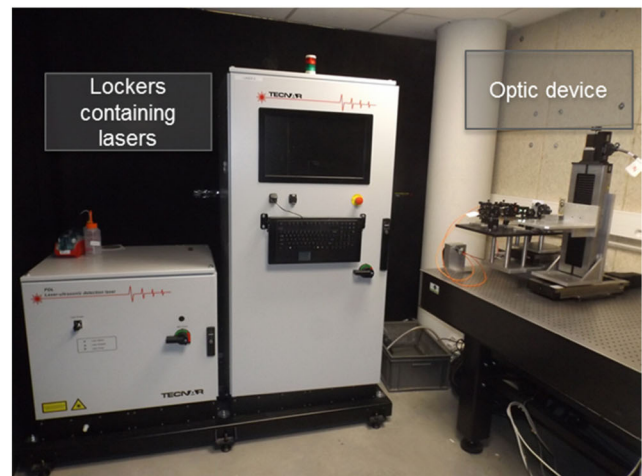
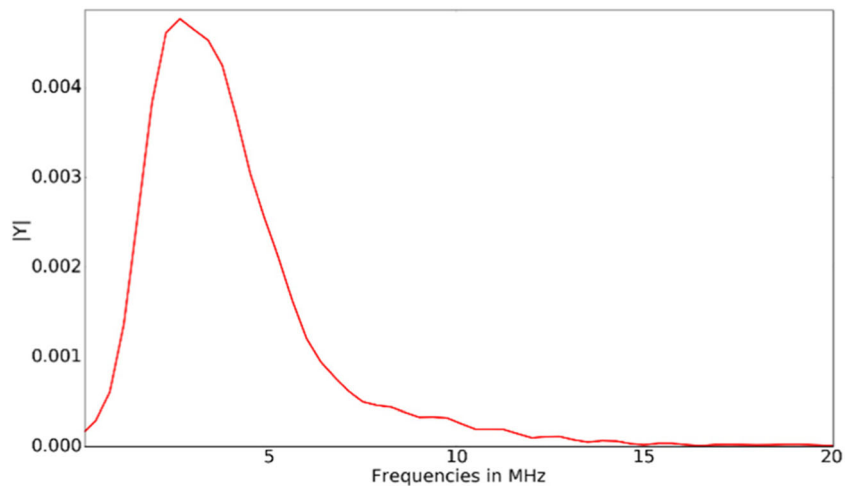
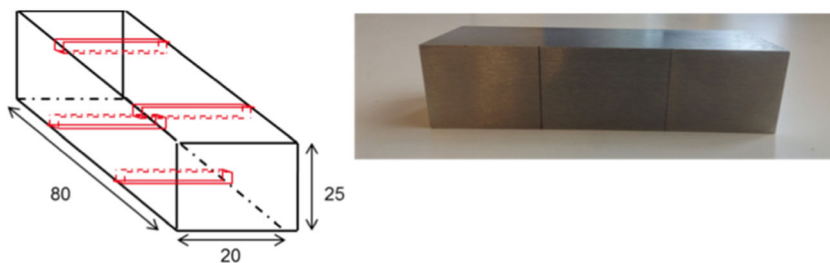


Fig. 10 Photos of the laser room: above the whole device and below the designed optical device

3.3 Pieces and flaws

To understand the origin of the different wave fronts and the impact of the different parameters on them (material, sample geometry, flaw dimensions, surface condition), we opted for

Fig. 11 Drawing of a sample on the left with machining notches (in red)—on the right, photo of a sample. Measurement in mm



simple geometry samples with polished surface and electrical discharge machining (EDM) notches. Specimens are 80 × 20 × 25 mm parallelepiped made in 316 L steel (Fig. 11).

One is manufactured by AM and one by forging in order to highlight any specific behavior an AM material could induce. There are four surface breaking EDM notches simulating notches in each sample. The dimensions of notches are given in Table 1. They are representative of the size of expected lack of fusion in AM.

4 Results

Figure 12 illustrates the probes configuration on the specimen. The pulsed generation (green triangle) is 3 mm away from the probe (red triangle). The scanning path is materialized by the dotted arrow. The system scans 45 mm of the surface sample.

The setup aims to monitor the Rayleigh wave propagating between the two lasers and the reflected Rayleigh waves.

Scanning of the sample gives data which allow B-scan representations. Those can be seen as a cross-sectional view of the sample. The time-of-flight of the ultrasound energy is displayed along the vertical axis, and the lasers position is displayed along the horizontal axis.

Figures 13 and 14 show B-scans obtained respectively on forging parts and AM parts.

Table 1 Notches dimensions of the samples

Sample	Fabrication process	FLAWS		
		Notches	Width (mm)	Depth (mm)
1	Forging	F0305	0.3	0.5
		F0105	0.1	0.5
		F0101	0.1	0.1
		F00501	0.05	0.1
2	AM	FA0305	0.3	0.5
		FA0105	0.1	0.5
		FA0101	0.1	0.1
		FA00501	0.05	0.1

The origin of each wave front on the B-scan must be properly identified before any interpretation. Figure 15 helps to read the B-scans; it is a diagram on which wave paths are schematized.

Horizontal wave fronts marked in blue on the diagram are the direct Rayleigh wave propagating along the surface between the two lasers. This wave front is the horizontal red line at 1 μs in Figs. 13 and 14. We expect a perturbation of this wave front when detecting a flaw. Indeed, we observed that the direct Rayleigh wave front is disrupted when the system of control is upright the flaw at x = 6 mm and x = 36 mm.

Blue dotted diagonal wave fronts are Rayleigh waves reflected by the notches. Those wave fronts are the second signature of flaw detection on B-scans. The reflected Rayleigh waves are observed on all B-scans (Figs. 13 and 14.)

We also note horizontal wave fronts marked in green; they are generated by the reflection of surface waves on the lateral edges of the work piece. Those waves are reflected by flaws and then generate parabolic wave fronts (green dotted parabolic wave fronts in Fig. 15). Consequently, they cannot be exploited to locate flaws in a generic case as they depend on piece geometry.

Gray horizontal wave fronts correspond to Rayleigh waves reflected between edges of the sample and notches.

Finally, the blue dark wave fronts in Fig. 15 are caused by the reflection of Rayleigh waves on to the edge of the samples.

From these results, it appears that the smallest machined notches (width 0.05 mm and depth 0.1 mm) in our samples are detected by our system for the two fabrication processes (Figs. 13 and 14). The detection limit of our system is lower than the smallest EDM notch.

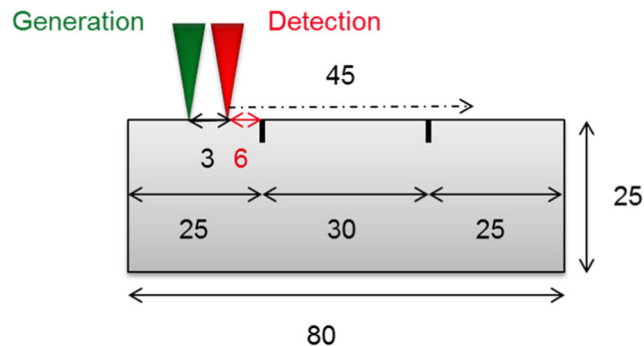
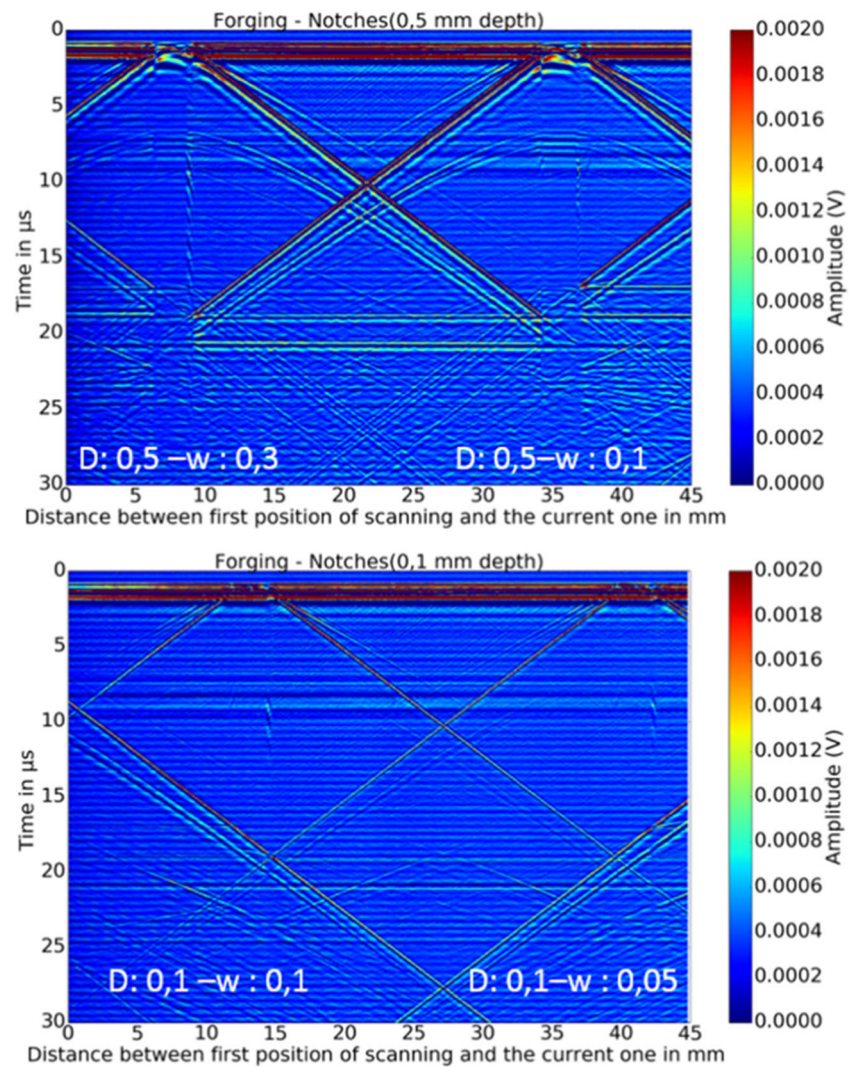


Fig. 12 Inspection setup—measurements in mm

Fig. 13 B-scans issues from scanning (from left to the right and from top to bottom) F0305, F0105, F00501, and F0101 notches—d stands for depth and w for width



We can go further on the interpretation of our results by trying to link notches' dimensions to the observations on B-scans. We can point out that the disruption of direct Rayleigh wave is more or less clear depending of notch depths. For 0.5 mm depth notch, the direct Rayleigh wave front is disrupted at 1 μs when the flaw is between generation and probe lasers. This interruption is not clearly visible when notch depth is 0.1 mm. Indeed, notch depth is then lower than the wavelength of the Rayleigh wave.

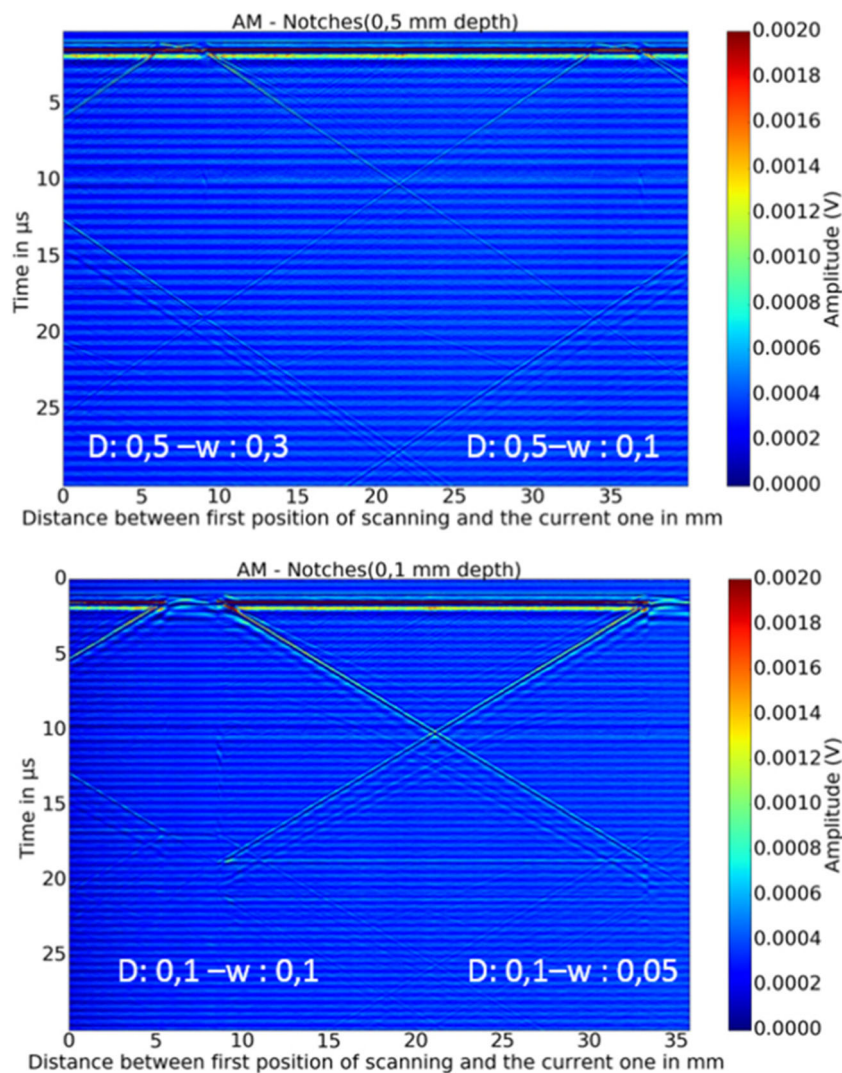
The spectrum presented in Fig. 9 shows that the main frequencies generated are around 3 and 6.5 MHz.

As Rayleigh wave's velocity in 316 L steel is approximately 2900 m/s at 20 °C, the corresponding Rayleigh wavelengths are between 1 and 0.5 mm. Lower amplitude is observed for notch depth lower than wavelength value. This observation is a first step to point out different wave behaviors linked to size notches, and it would be relevant to study the coefficient transmission of Rayleigh waves for each notches. Further experiments must be carried on to try to characterize size flaws.

Signal to noise ratio (SNR) from reflected Rayleigh wave is measured for each process and notches' size. Figure 16 shows reflected Rayleigh waves SNR for both forging and AM parts. The SNR is defined as the ratio of the maximum amplitude of the reflected Rayleigh wave and the mean amplitude value of the signal recorded in a time domain where there are no remarkable waves propagating.

We can notice that the amplitude of reflected Rayleigh wave varies with process fabrication and notch dimensions. We see that SNR obtained in forging samples are higher to the ones obtained with AM samples. The origin of the lower amplitude in AM parts could be attributed to the effectiveness of ultrasound generation or to attenuation caused by the structure of AM. Indeed, microstructure of AM is different from microstructure of forging [7]. The orientation of the grain and the grain size is completely different in AM. The grain growth orientation observed in AM is columnar, and the grain size could be tenth bigger than in forged samples as shown in Fig. 17.

Fig. 14 B-scans issues from scanning (from left to the right and from top to bottom) FA 0305, FA0105, F00501, and FA0101 notches—d stands for depth and w stand for width



Some research have already been done and shown that a grain size or orientation can be measured by means of the attenuation of laser ultrasonics [8, 9]. It means that wave propagation is affected by the grain dimensions and orientation. We have to pursue the study in order to confirm this explanation.

5 Conclusion

This paper introduced a LU control of machined notches whose dimensions are closed to the size of lack of fusion in DED. The influence of the shape and size of laser spots are highlighted by developed models and confirm by experimentations. They allow designing an optical device adapted to our applications. The conclusions of this paper can be summarized as follows:

- (1) The models show that a 0.2-mm spot diameter enables to generate and detect 15 MHz ultrasound frequency and give access to 0.1-mm size flaws.
- (2) The developed optical device allows detecting the smallest machined notch (0.1 mm depth and 0.05 mm width). The detection limit of our system is lower than the smallest EDM notch.
- (3) The flaws are detected thanks to the disruption of the direct Rayleigh wave and the reflected Rayleigh waves.

Further work will consist in the evaluation of AM sample roughness incidence on the detection performances of the method. Some interrogation still remains regarding the in situ LU control of DED process, such as the impact of the thermal gradient or the machine environment on wave propagation and detection. Nevertheless, the literature does not enlighten any major restraint on these aspects. Indeed, the thermal gradient induces by DED process [10] has an impact both velocity and attenuation of

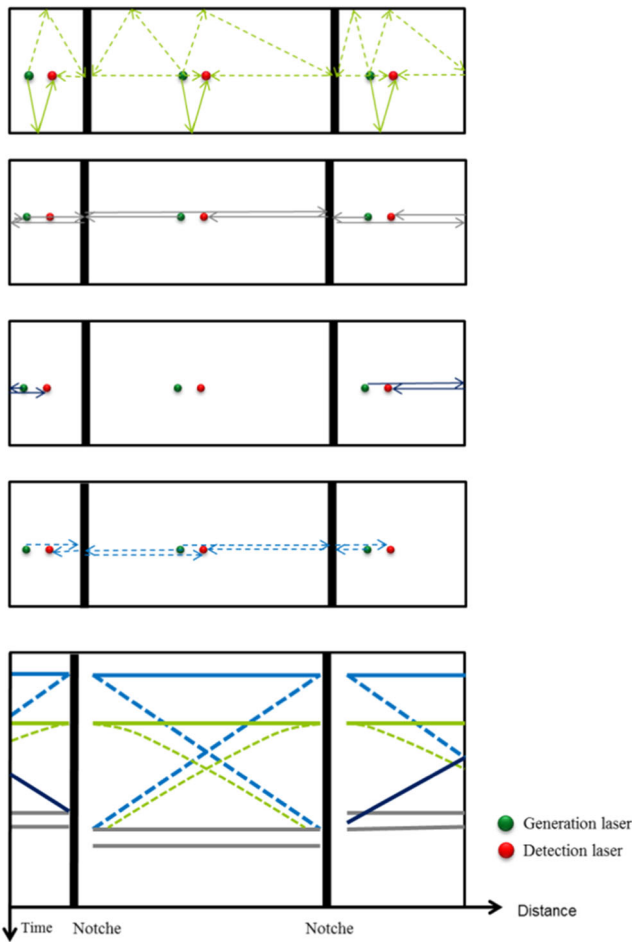


Fig. 15 On the top, diagram of part with the different paths represented, on the bottom, diagram of B-scan wave fronts

Rayleigh waves [11]. But this effect might be confined if the LU system is positioned away from the fabrication nozzle. Likewise, the literature on LU welding inspection [12] gives elements which supports the fact that the vibrations induced by the welding laser will not impact the performance, as their frequency range is not the same as the LU-generated frequencies.

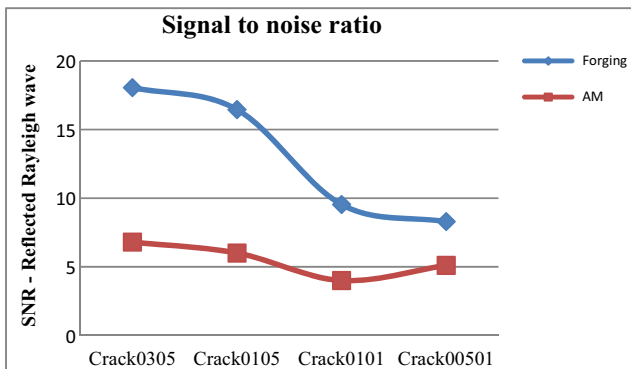


Fig. 16 Signal to noise ratio, in dB, for the reflected Rayleigh wave fronts

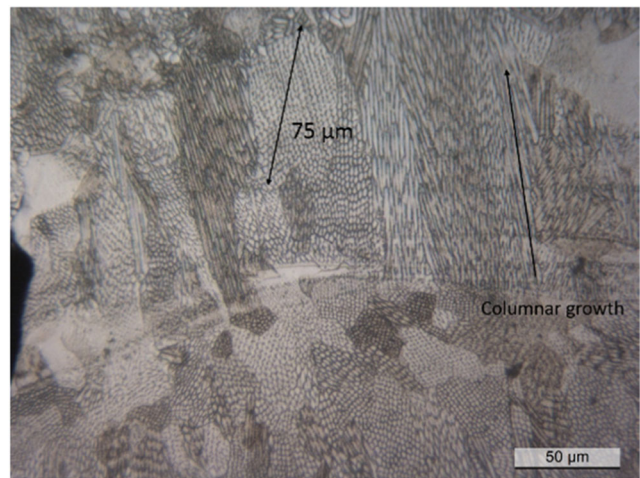


Fig. 17 Micrograph of a sample of 316 L made by DED process

References

- Gibson I, Rosen D, Stucker B (2015) Additive Manufacturing Technologies. Springer New York, New York, NY
- J. M. Waller, B. H. Parker, K. L. Hodges, E. R. Burke, et J. L. Walker, (2014) Nondestructive evaluation of additive manufacturing state-of-the-discipline report,
- Tapia G, Elwany A (2014) A review on process monitoring and control in metal-based additive manufacturing. J. Manuf. Sci. Eng 136(6):060801
- B. M. Sharratt, (2015) Non-destructive techniques and technologies for qualification of additive manufactured parts and processes,
- CERNIGLIA D, SCAFIDI M, PANTANO A, LOPATKA R (2013) Laser ultrasonic technique for laser powder deposition inspection. Laser 6(150):13
- Blouin A, Delaye P, Monchalain J-P, Roosen G (2001) Détection d’ultrasons par interférométrie adaptative dans des cristaux photoréfractifs. Instrum Mes Métrologie 1:127–141
- Xu X, Mi G, Luo Y, Jiang P, Shao X, Wang C (2017) Morphologies, microstructures, and mechanical properties of samples produced using laser metal deposition with 316L stainless steel wire. Opt. Lasers Eng 94:1–11, juill
- Militzer M, Garcin T, Poole WJ (2013) Measurements of grain growth and recrystallization by laser ultrasonics. Mater. Sci. Forum 753:25–30, mars
- Dong F, Wang X, Yang Q, Yin A, Xu X (2017) Directional dependence of aluminum grain size measurement by laser-ultrasonic technique. Mater. Charact 129:114–120, juill
- A. Longuet, C. Colin, P. Peyre, S. Quilici, et G. Cailletaud, (2006) Modélisation de la fabrication directe de pièces par projection laser: application au Ti-6Al-4V, in *Matériaux 2006*, p. 11–p
- Ruipeng G, Haitao W, Jianyan Z (2017) Non-contact detection of low carbon steel using laser generated ultrasound at high temperature. Opt. - Int. J. Light Electron Opt 136:536–542, mai
- Mi B, Ume C (2006) Real-time weld penetration depth monitoring with laser ultrasonic sensing system. J. Manuf. Sci. Eng. 128(1):280